

# Photobiology of corals from Brazil's near-shore marginal reefs of Abrolhos

David J. Suggett · Ruy K. P. Kikuchi ·  
Marília D. M. Oliveira · Saulo Spanó ·  
Rafael Carvalho · David J. Smith

Received: 2 February 2012 / Accepted: 13 March 2012 / Published online: 29 March 2012  
© Springer-Verlag 2012

**Abstract** Coral communities were examined from highly turbid near-shore marginal reefs of Abrolhos (Brazil) to test a paradigm previously developed from observations in clear water reefs; specifically, that coral photobiological properties follow a highly conserved linear relationship with optical depth ( $\zeta$ ) via preferential 'non-photochemical' over 'photochemical' dissipation of absorbed light energy. PAM fluorometry in situ was used to examine the photobiology of the most dominant coral species throughout the platform surfaces and bases of Abrolhos' characteristic 'chapeirões' reef framework; however, none of the species consistently adhered to the 'clear water paradigm'. PAM measurements further demonstrated that species conformed to two different strategies of non-photochemical energy dissipation: transient but relatively rapid for the two closely related endemic species (*Mussismilia braziliensis* and *Mussismilia harttii*) as opposed to more persistent for *Montastrea cavernosa*, *Porites astreoides* and *Siderastrea stellata*. Further experiments demonstrated that tolerance to anomalous stress amongst species did not correspond with the non-photochemical energy dissipation strategy present but was consistent with the relative dominance of species within the chapeirões coral communities.

---

Communicated by K. Bischof.

---

D. J. Suggett (✉) · D. J. Smith  
Coral Reef Research Unit, Department of Biological Sciences,  
University of Essex, Colchester CO4 3SQ, UK  
e-mail: dsuggett@essex.ac.uk

R. K. P. Kikuchi (✉) · M. D. M. Oliveira · S. Spanó ·  
R. Carvalho  
Coral Reef Research Laboratory, Universidade Federal da  
Bahia, CPGG/IGEO, Rua Caetano Moura 123,  
Federação, Salvador, 40210-340 Bahia, Brazil  
e-mail: kikuchi@ufba.br

## Introduction

Continued acclimation to a changing light environment (termed photoacclimation) is fundamental for maintaining optimum photosynthetic rates and in turn successful growth and competition of corals within reef systems. Primary mechanisms that operate across different temporal or spatial scales to drive coral photoacclimation are generally well described from discrete biological measurements, such as light-harvesting pigment and photosystem reaction centre concentrations (e.g. Falkowski and Dubinsky 1981; Brown et al. 1999) or physiological proxies, such as bio-optical assays (e.g. Ralph et al. 1999; Hennige et al. 2008); in turn, these measurements have enabled development and validation of models that examine broader scale variance of coral productivity (e.g. Anthony and Hoegh-Guldberg 2003). However, past studies have almost exclusively focused on examining coral photoacclimation properties from clear water but not marginal (sensu Kleypas et al. 1999) light environments, with only a few studies to date performed in shallow water flats and mangroves (Brown et al. 1999; Hennige et al. 2010; Piniak and Storlazzi 2008) and relatively turbid near-shore reefs (Anthony and Connolly 2004; Anthony et al. 2004; Hennige et al. 2008). Such potential observational bias is surprising given that understanding how corals presently acclimate to more extreme conditions could provide key insight for predicting how corals from presently non-marginal environments will likely respond to environmental change (Suggett and Smith 2011), for example, altered turbidity via changes in sedimentation.

Brazil's Abrolhos reef complex occurs ca. 17°20' to 18°10' S within strong environmental gradients between vast inshore mangrove-riverine systems and offshore oceanic waters (see Leão et al. 2003; Leão and Kikuchi 2005;

Kikuchi et al. 2010). Near-shore reefs here are characterized by environmental conditions considered far from those required for optimum coral growth (sensu Yentsch et al. 2002) and thus highly marginalized (Castro and Pires 2001; Leão et al. 2003). Notably, relatively high light attenuation persists year round from sediments discharged from rivers/coastal erosion and re-suspension from prevailing southerly winds (Leão and Dominguez 2000; Castro and Pires 2001; Leão et al. 2003; Segal et al. 2008); these physical processes and hence light attenuation are strongest in March (Leão et al. 2003; Costa et al. 2004; Dutra et al. 2006) and coincide when annual water temperatures have peaked (e.g. Fig. 1; see also Krug et al. 2012).

Light availability to Abrolhos' reefs is both highly temporally and spatially variable. The reef framework typically consists of both coalesced and isolated column pinnacles, with laterally spreading top platforms termed chapeirões (Leão and Kikuchi 2005). Therefore, in addition to strong seasonal change in light attenuation (Fig. 1), corals inhabiting the platforms are within only a few metres depth, whilst those deeper in the water column on the pinnacle sides are often shaded from direct light. As such coral viability here must be driven, at least in part, by strong photoacclimatory plasticity. However, aside from limited knowledge of zooxanthellae characteristics, such as cell and pigment concentrations, for corals from the Picãozinho coastal reef of northeastern Brazil (Costa et al. 2004, 2005, 2008), still little information exists describing fundamental photobiological properties of Brazil's corals inhabiting marginal systems.

Recent bio-optical measurements from corals across a continuum of light environments (depth and turbidity) in the Indo-Pacific have demonstrated that coral photobiological

patterns appear highly conserved (Hennige et al. 2008, 2010); specifically, (1) key parameters describing photoacclimation, for example, the intensity of light-saturated photosynthesis (termed  $E_K$ ) and the maximum rate of photochemistry (the electron transport rate, ETR), follow simple linear relationships with the optical depth ( $\zeta$ ), and (2) these relationships appear to be driven by a common process whereby the extent of 'non-photochemical' energy dissipation, measured as 'Stern–Volmer' non-photochemical fluorescence quenching, is modified across light environments (shallow–deep, clear–turbid) to always maintain a constant photochemical operating efficiency. Whilst this paradigm has been an important step in understanding the underlying properties governing broad scale coral photoacclimation, it is still unknown whether it extends to corals inhabiting even more extreme light environments.

As a first step to understanding the photobiology of corals from marginal light environments, we examined whether photoacclimation at Abrolhos reef sites adheres to the paradigm of Hennige et al. (2008) and reflects the relative success of coral species found here. Coral communities at Abrolhos are characterized by reasonably high coral cover and comprised of species considered both endemic, for example, *Mussismilia braziliensis*, *Mussismilia hispida*, and cosmopolitan for the Atlantic, for example, *Montastrea cavernosa*, (Leão et al. 2003; Leão and Kikuchi 2005; Kikuchi et al. 2010); however, it is the endemic *Mussismilia* spp. that appear to be not only the most successful species on the chapeirões' platforms but also amongst the most tolerant species in Abrolhos to anomalous light–heat stress conditions (e.g. Leão et al. 2008). As such, we specifically examined whether photobiological properties were the same for endemic and

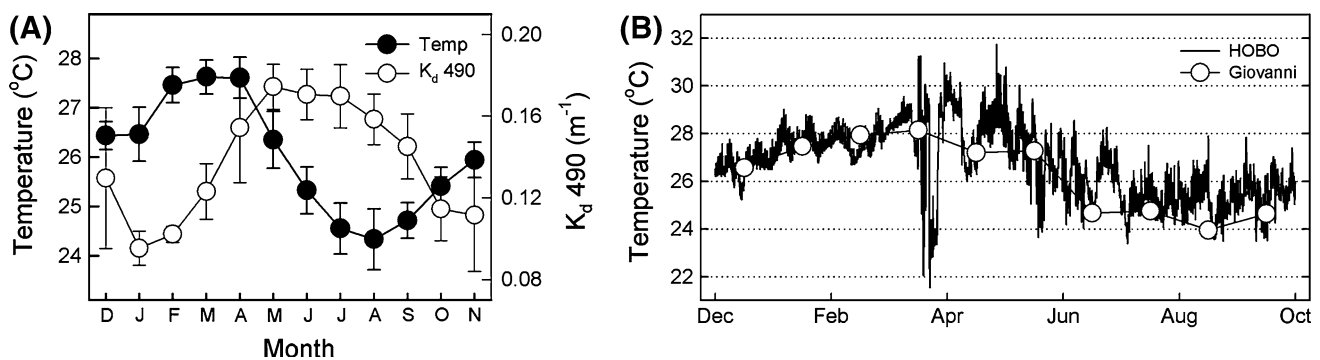


**Fig. 1** Environmental variability for the near-shore marginal reefs of Abrolhos: **a** mean monthly sea surface temperature (SST, °C) and light attenuation coefficient ( $K_d$  490,  $m^{-1}$ ) from 2001 to 2009. Data were produced with the Giovanni online system, developed/maintained by the NASA GES DISC: <http://disc.sci.gsfc.nasa.gov/giovanni> ocean colour radiometry SeaWiFS products. Monthly data were determined for an area of 17.56°–18.05°S and 38.29°–39.01°W, i.e. a grid for the near-shore environments encompassing the three sample sites studied here, Lixa (LIX), Pedra de Leste (PDL) and Ponte

Grande Sul (PGS), typically of ca. 60 cells; **b** Mean monthly SST and for (a) from December 2009–October 2010 overlaid with continuous SST data recorded (every 20 min) via a HOBO® logger (*Tempcon*, USA) positioned on the chapeirões' upper platform, ca. 3–4 m at PDL. This panel demonstrates SST variability within and between each month; notably, SST variability is enhanced for the rainy season (ca. April–October) compared with the preceding dry season, and anomalous SST cold spells in March–April as a result of upwelling water advecting from the south

cosmopolitan species via in situ measurements on the surface and bases of the chapeirões. We further supplemented these in situ observations with a laboratory-based experiment to evaluate whether any fundamental differences in photobiological characteristics were consistent with differences in susceptibility to anomalous light-temperature stress.

## Methods

### Site description

Three study sites around Abrolhos' inner Pedra Grande Reef complex were visited in November 2009: (1) Pedra da Leste (PDL, 17°46.55'S, 39°03.05'W; 12th Nov), (2) Ponte Grande Sul (PGS, 17°54.05'S, 38°55.22'W, 13th Nov), and (3) Lixa (LIX, 17°41.02'S, 38°57.92'W, 14th Nov). All three sites have been examined previously for environmental characteristics and benthic community structure (Castro et al. 2005; Leão and Kikuchi 2005; Dutra et al. 2006; Kikuchi et al. 2010). Notably, sedimentation rates are ca. 10–25 (PDL, LIX) and 5–7 (PGS) mg cm<sup>-2</sup> d<sup>-1</sup>. More than 75 % of all of Brazil's coral species can be found at these sites (Castro et al. 2005). Both upper platforms and lower bases of the chapeirões for each site were examined for coral community structure and photobiological characteristics via twice daily SCUBA dives (early morning and midday); sampling was eventually conducted across 2–3 (LIX) and 3–4 (PDL, PGS) chapeirões.

Light attenuation coefficients ( $K_d$ , m<sup>-1</sup>) were quantified at the start and end of each dive using a Photosynthetically Active Radiation (PAR) sensor coupled to a Diving-PAM (Pulse Amplitude Modulation) fluorometer (Walz, Germany; as described in Hennige et al. 2008). Since the shallow platforms potentially represented a different light environment than the platform bases, we independently measured light attenuation both over the platforms and down the sides of the platforms; however, values of  $K_d$  were not significantly different for the two habitats ( $n = 12$  for all sites; not shown). Values of  $K_d$  were higher at PDL ( $0.221 \pm 0.016$ , mean  $\pm$  standard error) than at LIX ( $0.166 \pm 0.022$ ) and PGS ( $0.133 \pm 0.018$ ) (ANOVA,  $p < 0.001$ ), and generally consistent with the different sedimentation rates across these sites previously reported (above). The product of  $K_d$  and depth (m) was then used to calculate the corresponding optical depths ( $\zeta$ , dimensionless) for each sample depth. Overall, values of  $\zeta$  ranged between ca. 0.25–2.5, which thus extended the depth range previously examined by Hennige et al. (2008) (ca. 0.6–2.6). Mean water temperature at the sampling depths was measured with HOBO loggers (Tempcon Inc., USA) during the dives and was constant with depth and site,  $25.6 \pm 0.3$  °C.

### Coral community structure and size-frequency

Standard continuous line intercept transects were used to quantify coral community structure as: (1)  $3 \times 30$  m transects, each separated by ca. 10–20 m, towards the chapeirões' lower base (ca. 8–11 m depth); and (2) two sides and the centre of three permanent quadrats, each measuring 20 m<sup>2</sup> (10 m  $\times$  2 m width) and separated by ca. 10–20 m, to yield a total of  $9 \times 10$  m transects on the chapeirões' upper platforms (ca. 3–4 m depth); this alternative approach for the upper platforms was required given the restricted continuous platform surface area. Data were recorded by high definition video (Sony HDR-SR1E) and later analysed to estimate habitat type as % live coral cover to species level. Species and dimensions (greatest height, length and width, cm) of all coral colonies were also measured within the upper platform quadrats. Coral colony size-frequency data were not collected from the platform bases since semi-continuous veneering *Montastrea cavernosa* largely dominated benthic cover. When categorizing colonies on a size basis, we only used the greatest width or length data to ensure some level of standardization amongst colonies often with markedly different growth forms.

### In situ photosynthetic physiology

A Diving-PAM fluorometer was used to determine the photosynthetic physiology of the most abundant coral species at the chapeirões' lower base and upper platforms. The instrument was set to deliver Rapid Light Curves (RLCs) following settings described previously (Hennige et al. 2008). Measurements were initially collected in the absence of actinic light followed by an increasing series of actinic light steps (of 20 s duration), from ca. 0 to 2,450  $\mu\text{mol photons m}^{-2} \text{ s}^{-1}$ . Key settings were: actinic light factor = 0.7, actinic intensity = 6, saturation width = 0.8, saturation intensity = 4, and signal damping = 2; the gain was altered between 2 and 3 depending on the sample. The saturation width was periodically checked but did not require alteration throughout. Independent colonies ( $n = 5$ ) of each species were examined per depth with the fibre-optic probe always placed on the uppermost surface parallel to the water surface; the PAR sensor of the Diving-PAM was maintained at the same plane as the coral surface being examined to also record the incident light intensity (E) during the RLCs. Measurements were always collected from the upper platforms during the early morning dive and from the platform bases during the midday dive; importantly, we evaluated all RLCs for possible artefacts associated with sampling the platform surfaces and bases at different times of day as follows:

Under conditions where  $E$  is typically  $< E_K$ , changes in fluorescence yields are almost entirely the result of photochemistry whilst those from NPQ should be minimal. Indeed, diel observations of variable fluorescence measurements from corals demonstrate that NPQ for  $E < E_K$  is (1) very closely coupled with  $E$  (and hence rapidly reversible) and (2) is a small fraction of the NPQ that cumulatively builds as  $E$  increasingly exceeds  $E_K$  (Gorbunov et al. 2001; their Fig. 3c). Therefore, we compared values of  $E$  with the resulting values of  $E_K$  (see below, Eq. 1) with the aim of rejecting any data that did not satisfy the criterion of RLC performed under actinic  $E < E_K$ . Overall, values of  $E$  were typically ca. 30–60 % of  $E_K$  throughout and no data were ultimately rejected. We do still acknowledge that complete diel removal of NPQ is still assumed without verification by direct additional measurements and is further considered in the discussion.

Initial RLC measurements in the absence of actinic light (and NPQ and thus under effective dark acclimated conditions, see also Hennige et al. 2008) yielded the minimum and maximum fluorescence yields, terms  $F_0$  and  $F_m$  (dimensionless), respectively. Measurements of the minimum and maximum fluorescence ( $F'$ ,  $F_m'$ , respectively) and of the effective photochemical efficiency, termed  $F_q'/F_m'$  (dimensionless), were subsequently determined for each light step of the RLC; this terminology follows recent designations (but is also consistent with that in Hennige et al. 2008) but note that  $F_q'/F_m'$  is the same as  $\Delta F/F_m'$  (see Cosgrove and Borowitzka 2010). Data were then fitted to a model describing the light ( $E$ ) dependency of the PSII photochemical efficiency using least squares nonlinear regression to yield values of the saturation light intensity and maximum photochemical efficiency (Suggett et al. 2003; Hennige et al. 2008):

$$F_q'/F_m' = [(F_q'/F_m'^{(\max)} \cdot E_K) \cdot (1 - \exp(-E/E_K))]/E \quad (1)$$

where  $E_K$  ( $\mu\text{mol photons m}^{-2} \text{ s}^{-1}$ ) is the saturation light intensity and  $F_q'/F_m'^{(\max)}$  (dimensionless) is the maximum PSII photochemical efficiency. Together,  $E_K$  and  $F_q'/F_m'^{(\max)}$  describe the (photo-) physiological acclimation state of the coral species across light environments, that is, turbidity and depth. Note that this terminology of  $F_q'/F_m'^{(\max)}$  differentiates from  $F_v/F_m (= (F_m - F_0)/F_m)$ , which is the measured maximum PSII photochemical efficiency under fully dark acclimated conditions; importantly,  $F_q'/F_m'^{(\max)}$  can provide an important proxy for  $F_v/F_m$  where an extended period of dark acclimation may not be possible (see Hennige et al. 2008) and/or where other physiological processes under low light and darkness, such as chlororespiration, deviate  $F_0$  and in turn  $F_v/F_m$  from their true values (Hill and Ralph 2008). In fact, our approach arguably provides a more accurate descriptor of  $F_v/F_m$

(e.g. Suggett et al. 2010), and thus, we subsequently adjusted  $F_q'/F_m'^{(\max)}$  with corresponding values of  $F_m$  (at  $E = 0$  of the RLC) to yield an improved estimate of  $F_0$  (our term  $F_0^*$ ), as  $F_0^* = F_m + [F_q'/F_m'^{(\max)} \times F_m]$ , for fluorescence quenching analyses:

Rapid light curves fluorescence yields were further analysed to determine the relative allocation of absorbed excitation energy to photochemical versus non-photochemical (heat dissipative) processes, that is,  $qP$  and  $qN$ , respectively; thus, for each light step,  $qP$  and  $qN$  were calculated as,

$$qP (F_q'/F_v') = (F_m' - F')/(F_m' - F_0') \quad (2)$$

(where  $F_0' = F_0^*/[(F_q'/F_m'^{(\max)}) + (F_0^*/F_m')]$ , modified from Suggett et al. 2003)

$$qN (F_v'/F_m') = (F_m' - F_0')/F_m' \quad (3)$$

$qN$  is similar to NPQ ( $F_m/F_m' - 1$ ), which is often the 'preferred' algorithm for quantifying non-photochemical heat dissipation (see Warner et al. 2010); however, we use  $qN$  here since it provides a closed comparison with  $qP$  (also referred to as the operating efficiency) as to how the photochemical efficiency is regulated (e.g. Lavaud et al. 2007), that is, the product of  $qN$  and  $qP = F_q'/F_m'$  (Cosgrove and Borowitzka 2010). We did repeat our analyses with NPQ and as expected observed the same trends as when using  $qN$  (not shown).

Relative rates of electron transport (ETR,  $\mu\text{mol electrons m}^{-2} \text{ s}^{-1}$ ) were determined as per Hennige et al. (2008) for each RLC light step from the product of  $F_q'/F_m'$ ,  $E$  and a constant factor to account for proportion of absorbed photons utilized by PSII ( $a_{\text{PSII}}$ ) and the assumption that the quantum yield electron transfer of a trapped photon within a reaction centre is 1 mol electron (mol photon) $^{-1}$  (see Suggett et al. 2010). We acknowledge that  $a_{\text{PSII}}$  can vary amongst *Symbiodinium* phylotypes and environmental condition (Hennige et al. 2009); therefore, we simply assumed the value of  $a_{\text{PSII}}$  as 0.5 (i.e. 50 % of absorbed light to PSII) for a strict comparison with the data from Hennige et al. (2008). A modified Jassby and Platt (1976) model describing the dependency of ETR upon  $E$  was subsequently fit using least squares nonlinear regression to determine values for the light-limited and light-saturated ETR,

$$ETR = ETR^{\max} \cdot (1 - \exp(-\alpha \cdot E/ETR^{\max})) \quad (4)$$

where  $\alpha$  (mol electrons (mol photons) $^{-1}$ ) and  $ETR^{\max}$  ( $\mu\text{mol electrons m}^{-2} \text{ s}^{-1}$ ) describe the light-limited and light-saturated ETR, respectively. Note that ETR here is strictly a relative ETR since it does not account for an absolute rate of light absorption (e.g. see Suggett et al. 2010).

## Light-temperature stress experiments

In order to further examine the stress tolerance on the chapeirões' upper platforms, small colonies of representative endemic (*M. braziliensis*, *M. hispida*, *S. stellata*; we note that the nature of *S. stellata* as endemic is debated but we follow the categorization according to Aronson et al. 2008) and cosmopolitan (*M. cavernosa*) coral species were taken from site LIX and returned to the indoor coral aquaria laboratory at Universidade Federal da Bahia (UFBA, Salvador). A total of 12 colonies per species (4 fragments from each of 3 separate colonies) were maintained for ca. 7 weeks at a mean maximum daily temperature and light intensity similar to that from where corals were collected in situ (ca. 300  $\mu\text{mol photons m}^{-2} \text{s}^{-1}$  and 26 °C) to ensure that removal and transportation to the laboratory had not significantly affected the corals' (photo)physiology; all fragments were periodically monitored using measurements of  $F_v/F_m$  by PAM fluorometry (settings as per Hennige et al. 2008). Light was provided by one 15 W 10,000 k fluorescent light (*Philips*) and one 15 W blue fluorescent light (*Boyu*) on a 12:12 light: dark cycle. Seawater was collected from the shore near to the laboratory to enable a 15 % water change twice daily (30L both at the beginning and end of the light period). Salinity was standardized to 35PSU with the addition of deionized water, and water quality parameters (pH, nitrate, nitrite, phosphate, alkalinity, dissolved oxygen and calcium content, Red Sea test kits) were measured after each change.

At the start of experimentation, the twelve colonies were each split across four tanks set to evaluate the susceptibility to light-temperature stress, that is,  $n = 3$  colonies per treatment: (1) ambient light (AL, 300  $\mu\text{mol photons m}^{-2} \text{s}^{-1}$ )-temperature (26 °C), that is, ambient light control, (2) AL-elevated temperature (30 °C), (3) low light (LL, 100  $\mu\text{mol photons m}^{-2} \text{s}^{-1}$ )-ambient temperature, that is, low light control and LL-elevated temperature; lower light intensity was achieved through use of neutral density filters. The low light and high temperature treatments were based on the mean reduction of  $K_d$  by a factor of ca. 2–3 times and highest water temperatures that occur during April–May, compared with when the samples were taken in November (see Fig. 1). Temperature was controlled by submersible heaters controlled with an external thermostat (*Full Gauge*) ( $\pm 0.1$  °C), and elevated temperature treatments were achieved by increasing the control temperature by ca. 0.5 °C per day (as per Oliver and Palumbi 2011).

All fragments were monitored for 12 days with PAM fluorescence measurements of  $F_v/F_m$  every 12 h; these measurements were made ca. 30 min after 'lights-on' and 'lights off' so as to minimize any contributions of diurnal (transient) NPQ and maximize consistency in quantifying  $F_v/F_m$  throughout. At each time point, three replicate

measurements were made randomly across the surface of each colony and averaged to provide a single measure per colony per time point. These data were then used to calculate a simple 'stress tolerance factor' based on similar approaches (Smith et al. 2008; Oliver and Palumbi 2011) that effectively determine the time taken for  $F_v/F_m$  to reduce to an arbitrary threshold. For our approach, 'stress' (St, %) was initially quantified as the change of  $F_v/F_m$  for each time point ( $t$ ) relative to that at the start of experimentation ( $t_0$ ),

$$\text{St}(t) = ((F_v/F_m)(t)/(F_v/F_m)(t_0)) \cdot 100 \quad (5)$$

Elevated temperature was considered the primary stressor, and therefore, we further subtracted the % stress at 30 °C ( $\text{St}_{30}(t)$ ) for each fragment from the corresponding % stress for the 26 °C 'control' ( $\text{St}_{26}(t)$ ); hence, the absolute impact of temperature stress ( $\text{St}^*(t)$ , %) =  $\text{St}_{26}(t) - \text{St}_{30}(t)$ . Since colonies for each species between the 30 and 26 °C tanks were not matched, we used the mean value of  $\text{St}_{26}(t)$  from the triplicate colonies (per species and treatment) for this correction. Final stress tolerance (ST, h) was subsequently calculated as,

$$\text{ST} = 75 \% / \Delta\text{St}^* \quad (6)$$

where  $\Delta\text{St}^*$  is the rate of change of  $\text{St}^*$  over time ( $\text{h}^{-1}$ ), as determined from a regression of  $\text{St}^*$  versus  $t$ , and 75 % is our arbitrary chosen threshold for St (since 75 % was approximately the highest sustained value by any of the fragments over the 12 day experiment); using this approach, lower values of ST are indicative of lower stress tolerance as a result of faster declines of  $F_v/F_m$  over time.

## Coral growth rates

At the end of experimentation, we sacrificed three randomly selected coral colonies from the elevated temperature treatments to further determine annual growth rates during life in situ; for this, skeleton density banding was examined (sensu Knutson et al. 1972) where a couplet of low and high banding seen in X-radiographies forms the annual growth. Fragments of each colony were cut in tablets along their central growth axis following Barnes and Lough (1989). *S. stellata* tablets were cut to 0.5 cm thick, and *M. braziliensis*, *M. hispida*, *M. harttii* and *M. cavernosa* were cut to 1 cm thick; these tablets were then X-rayed and the resulting images digitized. The optical density apparent in the radiographies is inversely proportional to the skeleton density hence clearer equals denser skeleton. In each image, annual growth was measured along three axes for at least 3 years back dated from the present, thus yielding growth per colony as the mean of 9 (3 axes  $\times$  3 years) measurements. Growth per species is reported as then mean growth from the 3 colonies.

## Results

### Coral community structure

In order to contextualize the photobiological observations, we initially considered the coral community structure across the sample sites. Coral cover on the platforms was lowest (ca. 13 %) at the most turbid site, PDL, compared with sites PGS and LIX (ca. 23 %), that is, a pattern consistent with the past observational studies for these sites (e.g. Kikuchi et al. 2010). Similar coral communities were observed on the chapeirões' platforms at all 3 sites (Table 1); notably, 65–75 % of the total live coral cover was dominated by the endemic species *M. harttii* and *M. braziliensis*, and 10–20 % by the cosmopolitan Atlantic species *M. cavernosa*.

Some differences in contribution to total live cover (Table 1, %) and of colony density per unit platform area (Table 2, colonies/20 m<sup>2</sup>) were observed between sites amongst the most common species, *M. braziliensis*, *M. cavernosa*, *M. harttii*, *P. astreoides* and *S. stellata*. The relatively least turbid site PGS was dominated by *M. harttii* (70 % of the total coral cover, 44 colonies/20 m<sup>2</sup>) with smaller contributions from *M. cavernosa* (9 % of the coral cover, 12 colonies/20 m<sup>2</sup>) and *M. braziliensis* (10 % of the coral cover, 4 colonies/20 m<sup>2</sup>); in contrast, the more turbid sites of PDL and LIX were characterized by a reduction of *M. harttii* (40–50 % of the coral cover, ca. 25–50 colonies/20 m<sup>2</sup>) and increased *M. braziliensis* (25 % of the coral cover, ca. 15–60 colonies/20 m<sup>2</sup>) and to a lesser extent *M. cavernosa* (10–20 % of the coral cover, 25 colonies/20 m<sup>2</sup>). Whilst *M. harttii* clearly still dominates the total live coral on the platforms across all of these sites, the increase in *M. braziliensis* and *M. cavernosa* at the higher turbidity sites may be indicative of differences in competitive ability with turbidity/environmental variability.

The higher growth rate for *M. braziliensis* and *M. cavernosa* (ca. 0.6 cm year<sup>-1</sup>) compared with *M. harttii* (ca. 0.2 cm year<sup>-1</sup>) at site LIX (Table 2) would support this notion.

As expected, differences in colony size accounted for much of the discrepancy between colony density per unit area (colonies/20 m<sup>2</sup>) and % cover on the platforms; for example, *M. braziliensis* exhibited relatively few (15 colonies/20 m<sup>2</sup>) but relatively large (mean size of 218 cm<sup>2</sup>) colonies at PDL compared with more (61 colonies/20 m<sup>2</sup>) but smaller (167 cm<sup>2</sup>) colonies at LIX and fewer (4 colonies/20 m<sup>2</sup>) but larger (717 cm<sup>2</sup>) colonies at PGS. As such, across all sites and for the most common species, the product of mean size (Table 2, adjusted to m<sup>2</sup>) and colony density (Table 2, density/20 m<sup>2</sup>) was closely correlated with their % cover (Table 1, % cover of each species normalized to % total live cover), with an adj.  $r^2 = 0.72$  ( $n = 15$ ,  $p < 0.005$ ; not shown); the associated regression equation was: [colonies per 20 m<sup>2</sup> × mean size] = 0.078 × % cover + 0.088.

In contrast to the platforms, the chapeirões' lower bases exhibited similar extents of total live coral cover across all sites (ca. 54 %; Table 1), which was a factor of ca. 2–4 higher than the extent of coral cover on the platforms; this coral cover was largely dominated by continuously veneering *M. cavernosa* (ca. 80–90 % of the total cover). Colonies of endemic *Mussismilia* species comprised only ca 5–15 % of the total live cover.

### In situ photobiology

We initially examined the depth dependency of photobiological parameters derived from the RLCs. Values of  $F_q'/F_m'^{(\max)}$  varied with  $\zeta$  following two (species-specific) patterns (Fig. 2). Values decreased linearly with  $\zeta$  for

**Table 1** Mean ± standard error (SE) percentage of coral cover on both the upper platforms (3–4 m) and lower bases (8–11 m) of chapeirões for sites Pedra da Leste (PDL), Ponte Grande Sul (PGS) and Lixa (LIX)

	PDL		PGS		LIX	
	Platform	Base	Platform	Base	Platform	Base
Live coral cover	13.1 ± 4.3	53.8 (4.6)	23.9 (2.9)	53.9 (6.3)	23.6 ± 4.3	53.3 ± 7.4
<i>Favia gravida</i>	2.3 ± 0.9	–	3.5 (1.9)	3.2 (3.2)	–	–
<i>Montastrea cavernosa</i>	18.5 ± 16.4	88.9 (10.1)	8.4 (3.9)	72.7 (8.0)	8.7 ± 2.3	84.4 ± 10.7
<i>Mussismilia braziliensis</i>	25.1 ± 3.4	1.9 (1.9)	9.8 (5.2)	1.9 (1.1)	23.5 ± 5.9	–
<i>Mussismilia hispida</i>	3.9 ± 3.9	–	4.0 (1.6)	5.0 (2.0)	10.3 ± 3.1	12.5 ± 7.0
<i>Mussismilia harttii</i>	39.2 ± 9.1	4.6 (2.7)	69.9 (15.3)	14.9 (13.9)	49.6 ± 7.2	0.6 ± 1.1
<i>Porites astreoides</i>	1.6 ± 3.0	1.9 (1.1)	1.4 (0.9)	0.6 (0.6)	0.9 ± 0.7	0.6 ± 1.1
<i>Siderastrea stellata</i>	9.4 ± 3.8	1.9 (1.1)	3.0 (1.3)	1.6 (0.7)	2.3 ± 1.0	1.3 ± 0.8
<i>Scolymia wellsi</i>	–	0.9 (0.5)	–	–	–	0.6 ± 1.1

Live coral cover is expressed as a % of the total benthic cover; individual species cover is further expressed as a % of the total live coral cover

**Table 2** Number of coral colonies (no.) and colony size range (mean, min–max; cm<sup>2</sup>) within the 20 m<sup>2</sup> belt transects on the chapeirões' upper platforms at the 3 sample sites

	No. colonies (per 20 m <sup>2</sup> )			Colony size range (mean, min–max; cm <sup>2</sup> )			Growth rate (cm year <sup>-1</sup> )
	PDL	PGS	LIX	PDL	PGS	LIX	
<i>M. braziliensis</i>	15 ± 2	4 ± 1	61 ± 8	218, 28–1,050	717, 36–5,248	167, 4–1,520	0.65 ± 0.16
<i>M. cavernosa</i>	25 ± 3	12 ± 6	26 ± 9	180, 20–837	169, 9–1,216	210, 9–2,310	0.62 ± 0.30
<i>M. harttii</i>	23 ± 4	44 ± 8	48 ± 9	129, 15–700	341, 12–1,520	134, 6–1,160	0.21 ± 0.16
<i>P. astreoides</i>	5 ± 1	3 ± 2	12 ± 6	56, 9–144	104, 16–170	17, 8–24	nd
<i>S. stellata</i>	6 ± 2	6 ± 1	31 ± 3	42, 6–165	37, 6–104	58, 4–480	0.20 ± 0.17

Also, growth rates determined from the main coral species used for the subsequent stress experiments (site LIX only, see main text). Data shown for no. colonies and growth rate are the mean ± standard error from the replicate belt transects and all colonies sampled, respectively;

nd indicates no data

*M. braziliensis* and *M. harttii* such that  $F_q'/F_m'^{(\max)} = 0.0455 \times \zeta + 0.5867$  (adj.  $r^2 = 0.810$ ,  $n = 10$ ,  $p < 0.005$ ); both the slope and intercept of this trend were equivalent to those for the previous Hennige et al. (2008) *Porites* data (indicated as dashed lines in Fig. 2) that were from a more restricted  $\zeta$  (Analysis of Covariance, ANCOVA, to test for significant differences between regression slopes,  $t_{df=12} = 0.618$  was not  $> t_{0.05,(2),12} = 2.179$ ; not shown).  $F_q'/F_m'^{(\max)}$  decreased nonlinearly with  $\zeta$  for all other species (*M. cavernosa*, *P. astreoides* and *S. stellata*) and deviated substantially from the trend for Hennige's *Porites* data, even at relative depth ( $\zeta \leq$  ca. 1.25).

In contrast to  $F_q'/F_m'^{(\max)}$ , values of  $ETR^{\max}$ ,  $\alpha$  and  $E_K$  are indicative of actual photochemical capacity (e.g. Suggett et al. 2010). Both  $\alpha$  and  $E_K$  followed the same linear relationships (slope and intercept) with  $\zeta$  as for Hennige's *Porites* data within the same  $\zeta$  range of 2.5–0.6, (ANCOVA  $t_{df=20} = 1.361$  and 1.118 for  $\alpha$  and  $E_K$ , respectively, were not  $> t_{0.05,(2),20} = 2.086$ ; not shown); however,  $\alpha$  decreased and  $E_K$  increased nonlinearly with  $\zeta$ , notably where  $\zeta$  was  $\leq$  ca. 0.6 (Fig. 3). Maximum electron transport rates,  $ETR^{\max}$ , also followed the trend with  $\zeta$  as for Hennige's *Porites* data (ANCOVA  $t_{df=30} = 0.438$  is not  $> t_{0.05,(2),30} = 2.042$ ; data not shown) throughout the entire  $\zeta$  range (Fig. 2).

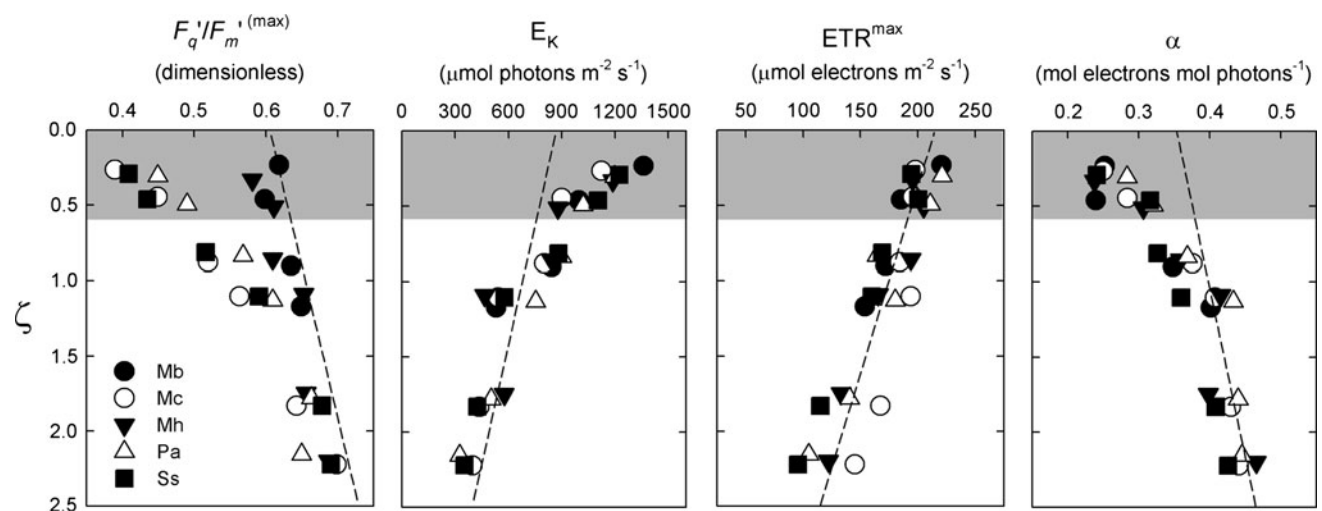
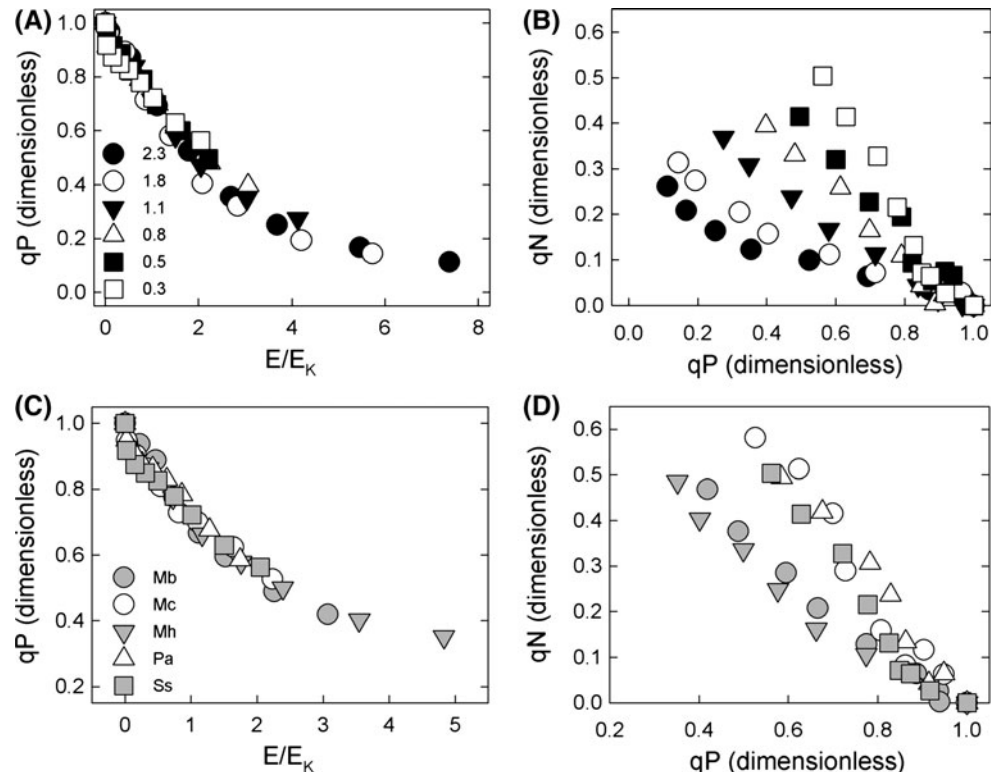


**Fig. 2** Values of PAM fluorescence derived PSII photobiological properties,  $F_q'/F_m'^{(\max)}$  (maximum photochemical efficiency, dimensionless), and  $E_K$  (the saturation light intensity,  $\mu\text{mol photons m}^{-2} \text{s}^{-1}$ ) from Eq. 1, and light-limited ( $\alpha$ , mol electrons [mol photons]<sup>-1</sup>) and light-saturated ( $ETR^{\max}$ ,  $\mu\text{mol electrons m}^{-2} \text{s}^{-1}$ ) ETR from Eq. 4 versus optical depth ( $\zeta$ , dimensionless). Each data point is the mean of replicate ( $n = 5$  measurements each from a different colony of Mb (*Mussismilia braziliensis*), Mc (*Montastrea cavernosa*), Mh (*Mussismilia harttii*), Pa (*Porites astreoides*) and Ss (*Siderastrea stellata*) for

two depths each at sites PDR, PGS and LIX (see main text); corresponding values of standard error are not shown for figure clarity but were 3–5 % ( $F_q'/F_m'$ ,  $E_K$ ,  $\alpha$ ) and 4–7 % ( $ETR^{\max}$ ) of the mean. Dashed line indicates the regression determined between these same variables but for *Porites lutea* in clear and turbid waters (Hennige et al. 2008);  $\zeta$  range for this previous data set was ca. 0.6–2.6 and thus the greyed out box indicates  $\zeta$  for which photoacclimation properties were not previously examined

**Fig. 3** Examples of the rapid light curve (RLC)-derived light response functions for **a–b** *Siderastrea stellata* from across the range of optical depths ( $\zeta$ ); and **c–d** all species, Mb (*Mussismilia braziliensis*), Mc (*Montastrea cavernosa*), Mh (*Mussismilia harttii*), Pa (*Porites astreoides*) and Ss (*Siderastrea stellata*) at a single optical depth ( $\zeta$ ) of ca. 0.5 (platform at LIX). **a** and **c** are the photochemical quenching coefficient ( $qP$ , dimensionless) versus  $E$  normalized to  $E_K$  (dimensionless, determined from Eq. 1) whilst **b** and **d** are the non-photochemical quenching coefficient ( $qN$ , dimensionless) versus  $qP$ . Each data point is the mean of replicate ( $n = 5$ ) measurements each from different colonies per species and depth; again corresponding values of standard error are not shown for figure clarity but were all 3–6 % of the mean



Rapid light curves were further examined to evaluate how absorbed excitation energy was dissipated via photochemical ( $qP$ ) relative to non-photochemical ( $qN$ ) dissipation (Fig. 3); firstly, the responses of  $qP$  and  $qN$  were considered relative to changes in optical depth (e.g. *S. stellata*, Fig. 3a). Values of  $qP$  were plotted against  $E$  relative to  $E_K$  to remove site-specific differences in spectral light quality, etc. (Hennige et al. 2008) and indeed confirmed existence of a common pattern of  $qP$  versus  $E/E_K$  for data from all optical depths. Hence, corals adhere to the paradigm described by Hennige et al. (2008), that is, corals acclimate to maintain a constant photochemical pressure on PSII, independent of  $\zeta$  (Fig. 3a). Maintenance of the constant  $qP$  versus  $E/E_K$  appeared to be achieved by increased investment into  $qN$  (per unit  $qP$ ) with decreasing  $\zeta$  (Fig. 4b).

Secondly, this analysis was repeated between species for a single  $\zeta$  (e.g.  $\zeta = 0.5$ , Fig. 3c) and again demonstrated that  $qP$  versus  $E/E_K$  followed a single pattern and thus independent of species. However, in subsequently comparing  $qP$  versus  $qN$ , two species-specific groups were observed (Fig. 3d); these groups were the same as those observed when previously examining  $F_q'/F_m'^{(\max)}$  versus  $\zeta$  (Fig. 2, above) of *M. braziliensis* and *M. harttii* versus all other species. Specifically *M. braziliensis* and *M. harttii* exhibited a much higher (short term) build up of  $qN$  per unit  $qP$  than the other species examined.

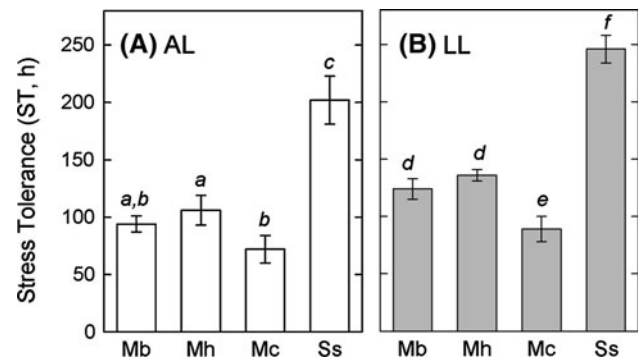


**Fig. 4** Mean ( $\pm$  standard error,  $n = 3$ ) values of stress tolerance (ST, h) as determined from Eq. 6 (see main text) for Mb (*Mussismilia braziliensis*), Mc (*Montastrea cavernosa*), Mh (*Mussismilia harttii*) and Ss (*Siderastrea stellata*) fragments collected from the coral platforms at LIX. Values of ST were determined for corals maintained under **(a)** ambient light intensity (AL,  $300 \mu\text{mol photons m}^{-2} \text{s}^{-1}$ ), i.e. representative for November when corals were sampled, and **(b)** relatively low light intensity (LL,  $100 \mu\text{mol photons m}^{-2} \text{s}^{-1}$ ), that is, representative for March–April when waters are warmest but light availability reduced (see main text). Letters indicate post hoc Tukey test groupings from an ANOVA performed across each of the AL (groupings a–c,  $F_{3,11} = 148.53$ ) and LL (groupings d–f,  $F_{3,11} = 56.85$ ) data

#### Species-specific stress responses

We finally examined whether differences in photoacclimation strategy between species (i.e. *Mussismilia* species versus non-*Mussismilia* species) conformed with ability to



tolerate anomalous stress; Values of our stress susceptibility factor (ST, Eq. 6) from ambient light conditions (AL) demonstrated that *M. cavernosa* and *S. stellata* appeared to stress most quickly (ca. 70 h) and slowly (ca. 200 h), respectively (Fig. 4a); the two *Mussismilia* species exhibited intermediate values (ST of ca. 130 h). As expected, light intensity played a moderating role and ST was increased by a factor of ca. 20–40 % across all species with the lower light intensity treatment (Fig. 4b). Thus, the same species groupings were not observed for stress tolerance as for the previous RLC analyses of photoacclimation.

## Discussion

### Photoacclimation patterns amongst coral species

Rapid light curve-derived photoacclimation patterns observed for Abrolhos' corals generally deviated from those previously observed for massive Indo-Pacific coral species (Hennige et al. 2008) from clearer waters (but of generally lower optical depths). The optical depth dependency of the maximum photochemical efficiency ( $F_q'/F_m'^{(\max)}$ ) for the *Mussismilia* species was different to that of all other species examined. However, the trend of  $F_q'/F_m'^{(\max)}$  versus  $\zeta$  for *M. cavernosa* at Abrolhos also appears to deviate with recent observations by Lesser et al. (2010) for this species: if we assume a  $K_d$  of 0.1 for clear water reefs (providing a range of  $\zeta$  of 0.3–9.1,  $F_v/F_m$  decreases linearly with  $\zeta$  (Lesser et al. 2010) compared with the nonlinear decrease in  $F_q'/F_m'^{(\max)}$  with  $\zeta$  that we observe (Fig. 2).

One important consideration before discussing such trends further is that any depth dependency of  $F_q'/F_m'^{(\max)}$  will be regulated according to NPQ. A key assumption with our approach was that NPQ was minimized where  $E$  was  $<E_K$  at all depths and specifically that corals examined during the noon dive (deeper samples) did not experience greater build up of more slowly reversible NPQ than those examined during the morning dive (platform samples). Unfortunately, data for Abrolhos' corals are not presently available to test this assumption. However, any greater accumulation of NPQ in the deeper samples would in fact result in an underestimation of  $F_q'/F_m'^{(\max)}$  and in turn the rate of change of  $F_q'/F_m'^{(\max)}$  with  $\zeta$ . Thus, not meeting our current assumption would only affect the slope of the trends(s) observed with optical depth and not the outcome of our observations (i.e. potential deviation from the previous trend observed by Hennige et al. 2008 for some species examined here).

Divergence in trend of  $F_q'/F_m'^{(\max)}$  versus  $\zeta$  amongst species highlights that corals have likely adapted to (or succumb to stress in) these marginal environments via different photobiological properties. Values of the maximum PSII photochemical efficiency (and hence  $F_q'/F_m'^{(\max)}$ ) under dark acclimated conditions signify the potential efficiency with which absorbed light is utilized for photochemistry (Suggett et al. 2009). Photoacclimation processes that increase the probability of heat dissipation of excitation energy, for example, large antennae sizes and incorporation of 'photoprotective' pigments will inevitably decrease the photochemical efficiency (Suggett et al. 2004, 2009). Such changes can occur as a result of acclimation within *Symbiodinium* phylotypes (Hennige et al. 2009; Suggett et al. 2009) or in the case of corals may reflect selection of different *Symbiodinium* phylotypes (Hennige et al. 2009, Suggett and Smith 2011). Whilst virtually no *Symbiodinium* phylotype descriptions exist for Brazil's corals (Costa et al. 2008) with which to evaluate this divergence in trend of  $F_q'/F_m'^{(\max)}$  versus  $\zeta$  amongst species, *M. harttii* and *M. brazilensis* have been observed to exhibit similar *Symbiodinium* cell concentrations but of higher chlorophyll per cell than *S. stellata* at a northeastern reef site (Costa et al. 2004, 2005). Such different properties may indeed be indicative of alternative phylotypes (Hennige et al. 2009) or acclimation plasticity based on light (micro-)environment modification by the host coral.

Decreased photochemical efficiency ( $F_q'/F_m'^{(\max)}$ ) is also diagnostic of recent stress in the surface waters and may in part reflect incomplete longer term repair of PSII damage induced over previous days (e.g. Gorbunov et al. 2001), and again may be attributable to the presence of specific *Symbiodinium* phylotypes or host coral light environment properties. However, analyses of other photobiological parameters derived from the PAM approach likely discount this possibility; specifically, the continued increase in both  $ETR^{\max}$  and  $E_K$  with decreasing  $\zeta$  clearly signifies that stress is not the primary factor moderating the trends of  $F_q'/F_m'^{(\max)}$  with  $\zeta$  (see also Hennige et al. 2008). In fact, the continued linear dependency of  $ETR^{\max}$  with  $\zeta$  into extremely low values of  $\zeta < \text{ca. } 0.6$  is likely achieved via enhanced energy investment into photoprotection since  $E_K$  and  $\alpha$  simultaneously increase and decrease, respectively (but nonlinearly); note that this threshold of  $\zeta < \text{ca. } 0.6$  is not simply representative of above and below platform environments since data from the platform at site PDL were from  $\zeta$  of 0.8–0.9 and hence  $\zeta > 0.6$ . Instead, it is plausible that general turbidity combined with highly physically dynamic environments at all three sites inherently increases the variability in incident light per unit area/time (e.g. Anthony et al. 2004; Piniak and Storlazzi 2008,

see also Fig. 1 contrasting rainy and dry seasons), an effect that would likely be exacerbated on the shallow platforms. Increased variance, for example, contrasting the response of microalgae adapted to estuarine versus open environments (Lavaud et al. 2007) does appear to result in enhanced investment in ‘photoprotection’, and in turn increased  $E_K$ , presumably to minimize the cost of photo-repair to continued high light damage. Such a response would be consistent with our photobiological data but requires verification, in particular since ETRs used here are relative and thus do not account for how changes in light absorption may indeed further modify patterns of  $ETR^{\max}$  (and  $E_K$ ,  $\alpha$ , etc.).

Overall, the depth dependency of  $F_q'/F_m'^{(\max)}$  (and in turn  $ETR^{\max}$ ,  $E_K$  and  $\alpha$ ) therefore appears to be driven by photoacclimation, and specifically those processes such as pigment synthesis that occur over relatively longer time scales (hours–days) (e.g. Suggett et al. 2009). Importantly, the same species-specific groupings were observed when comparing  $qN$  and  $qP$  in surface waters (Fig. 3) as for  $F_q'/F_m'^{(\max)}$  versus  $\zeta$  (Fig. 2); however, changes in  $qN$  are driven by processes operating over much more rapid time scales (seconds–minutes), such as xanthophyll cycling and decoupling of antennae complexes from the core reaction centres (e.g. Gorbunov et al. 2001, see also Warner et al. 2010). Therefore, together these data clearly demonstrate that *M. braziliensis* and *M. harttii* (relatively small reductions of  $F_q'/F_m'^{(\max)}$  and high reduction of  $qN$  per unit  $qP$  in surface waters) have evolved a photoacclimation strategy that relies on transient and relatively rapid non-photochemical energy dissipation. In contrast, *M. cavernosa*, *P. astreoides* and *S. stellata* employ an alternative strategy based on preferentially investing in longer term persistent photoprotection, which presumably therefore offsets a need for transient non-photochemical energy dissipation signified by  $qN$ .

Existence of alternative strategies of non-photochemical energy dissipation by corals within the same community is difficult to explain and we are not aware of such a phenomenon having been observed previously. It is clear that these two strategies are not related to evolutionary isolation and hence whether corals are considered endemic since the photobiology of *S. stellata* (endemic, Aronson et al. 2008) conforms to that of the cosmopolitan *M. cavernosa* and *P. astreoides*. Similarly, whilst *Mussismilia* species (Favidae) are genetically separated from *P. astreoides* and *S. stellata*, they are closely related to *M. cavernosa* (also Favidae) (see Fukami et al. 2008). An ‘evolutionary’ explanation may still hold, for example, via species specificity towards algal symbionts with different photobiological properties; however, unfortunately it is beyond our current data set to determine the underlying basis for this species-specific divergence of photoacclimation strategy.

## Coral viability in Abrolhos’ marginal waters

Whilst photoacclimation processes clearly contribute to the success of corals to withstand fluctuating (light) environments (e.g. Anthony and Connolly 2004), overall investment into autotrophy, such as  $ETR^{\max}$ , is not a useful indicator of their subsequent ecological success (see Henige et al. 2008). Coral cover observed for the chapeirões’ platforms (ca. 13–23 %) in Abrolhos’ marginal systems, where values of  $K_d$  are ca. 0.15–0.25, is generally consistent with a previously reported relationship between coral cover and turbidity (see Yentsch et al. 2002; Fig. 5); hence, turbidity restricts coral cover via lower achievable growth rates (e.g. Yentsch et al. 2002; Anthony and Connolly 2004) more for PDL than the other two sites. However, we sampled in November when  $K_d$  is close to the seasonal minimum and thus waters are in fact clearest (e.g. Fig. 1); our restricted temporal sampling period is perhaps not meaningful when considering the influence of light availability upon coral cover/growth, which occurs a scale of months–years. Therefore, we further considered coral cover relative to the annual mean  $K_d$ : Remote sensing derived values of  $K_d$  (Fig. 1) are lower than ours determined in situ but demonstrate that the annual mean  $K_d$  (= 0.135) is ca. 20 % higher than the  $K_d$  typical for November (ca. 0.114). Increasing our in situ  $K_d$  values by 20 % to ca. 0.158 (PGS) and 0.197 (LIX) and 0.261 (PDL) would yield values of  $K_d$  for this system that are even higher relative to the % cover expected following the Yentsch et al. (2002) relationship (Fig. 5), and thus, net coral growth at Abrolhos is strongly decoupled from light availability.

Yentsch’s relationship between % cover and  $K_d$  also conformed to their data describing the change of compensation depth (Fig. 5), where net photosynthesis is equal to respiration ( $P = R$ ), with  $K_d$ . Thus, our data would demonstrate that corals from the shallow platforms exist at a relatively ‘deeper’ depth than would be expected for any given  $K_d$  if photosynthesis was the major factor regulating coral growth. As such, corals at Abrolhos must inevitably rely significantly upon respiration (heterotrophy) to fuel net growth, albeit of a low growth rate, in such extreme low light environments (e.g. Anthony and Connolly 2004; Lesser et al. 2010).

Adaptation to extremely reduced light availability is further evident when examining the coral cover on the bases of the lower platforms, which was almost exclusively dominated by *M. cavernosa* across all sites. Total coral cover here was extremely high (ca. 50–55 %) for all sites relative to values of  $K_d$  (Fig. 5). Therefore, whilst *M. cavernosa* plays a somewhat secondary role to reef framework development on the platform surfaces, it plays a primary role on the platform bases and can clearly thrive

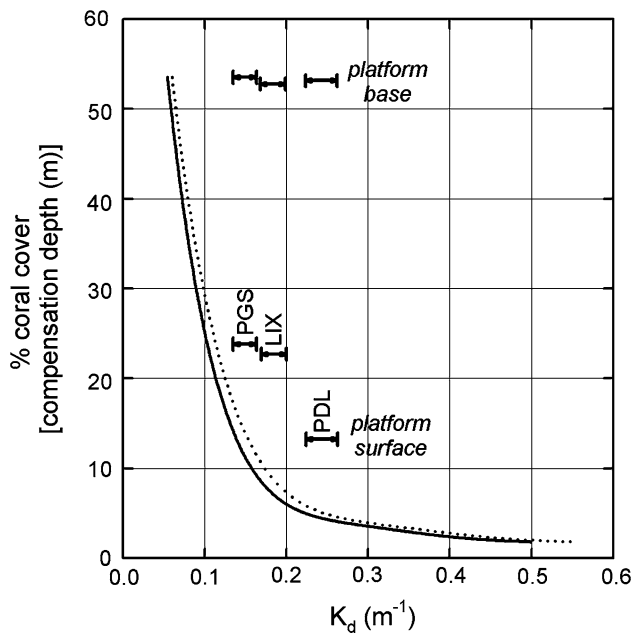


**Fig. 5** Relationship between coral cover (%) and  $K_d$  ( $\text{m}^{-1}$ ) for the three Abrolhos sites (LIX, PDL, PGS) and for both the upper and lower bases of the platforms; the range of  $K_d$  for each % cover represents the range expected for each site between the dry season, when waters are clearest and  $K_d$  lowest, and the rainy season, when waters are most turbid and  $K_d$  highest (see Fig. 1 and main text). Abrolhos data are overlaid onto the relationship describing the dependency of coral cover upon  $K_d$  from Indonesia reefs (redrawn from Yentsch et al. 2002) (solid line). Values of  $K_d$  from Yentsch were further adjusted to account for the difference between  $K_d$  from secchi depth ( $K_{d(\text{SD})}$ ) and from PAR ( $K_{d(\text{PAR})}$ ), where  $K_{d(\text{PAR})} = K_{d(\text{SD})} \times 1.102$  (Devlin et al. 2008); the relationship between coral cover and adjusted  $K_d$  is given by the dashed line. Note that the relationships of % cover and  $K_d$  also apply to data comparing the compensation depth (m) and  $K_d$  ( $\text{m}^{-1}$ ) for the Yentsch et al. (2002) West Florida data

across the extreme light environments between surface and depth. *M. cavernosa* is well known to be a dominant coral species in Caribbean reef systems, including low light mesophotic environments (Lesser et al. 2010 and references therein); in the Caribbean, *M. cavernosa* not only relies on an upregulation of heterotrophy but also a switch of *Symbiodinium* sp. genotype under low light, and thus processes that can both have important impacts on the effective photobiological properties and physiological performance of corals (see Suggett and Smith 2011). Future knowledge of not only the metabolic balance between photosynthesis and respiration but also the role of the *Symbiodinium* sp. genotype in regulating coral growth within and between Abrolhos' extreme light environments is thus essential.

Relatively high coral cover for both the chapeirões' platforms (coupled with relatively slow growth rates) would perhaps also suggest that the most dominant species here, *M. braziliensis* and *M. harttii*, should be most tolerant

to anomalous stress. Indeed, the few in situ observations during light and/or heat stress events that exist suggest that these endemic *Mussismilia* species exhibit a low susceptibility to bleaching and bleaching-induced mortality (Castro and Pires 2001; Leão et al. 2003, 2008; Kikuchi et al. 2010). Our measures of the relative stress susceptibility (ST) demonstrated that these species were somewhat stress tolerant (even though *Mussismilia* were not the most stress tolerant species); *S. stellata* is known to be highly resistant to light–heat stress anomalies (e.g. Costa et al. 2008) although in situ observations from Abrolhos suggest that this species should be no more resistant than the *Mussismilia* species (Leão et al. 2008).

Given the observations from the stress experiments, it is clear that the divergence in 'strategy' of non-photochemical energy dissipation amongst species does not correspond with any obvious benefit to tolerating anomalous stress, that is, preferential investment into more persistent as opposed to transient processes of photoprotection (above). Of course, we cannot discount potential seasonal acclimation in further moderating these trends given that our anomalous stress experiments were conducted at only one time of year (when waters were coolest). Even so, the more stress tolerant nature of endemic species therefore likely explains their dominance on the platform surfaces; endemic evolution within highly variable environments, such as Abrolhos' marginal reefs, may have equipped corals with enhanced tolerance to transient stress (e.g. Oliver and Palumbi 2011; Suggett and Smith 2011). In contrast, the more stress susceptible nature of *M. cavernosa* likely contributes to restricting the competitive dominance of this species to the platform bases where the lower light may afford some resistance to anomalous light–heat stress events.

## Conclusions

Our novel initial investigation of coral photobiology from Abrolhos' reefs has demonstrated that coral species diverge from the uniform photoacclimation strategy observed previously (in more optimum light environments, Hennige et al. 2008) via two alternative 'strategies' for dissipating non-photochemical energy. Given that the Hennige et al. (2008) data were somewhat restricted in terms of depth ( $\zeta = \text{ca. } 0.6\text{--}2.6$ ), species (4 species of massive coral) and location (two adjoining reef sites), it is unclear to what extent our observations from Abrolhos highlighting more than one photoacclimation strategy exists across other hard coral communities and fundamentally which strategy is more common. Differential tolerance to anomalous stress (tested here as heat stress) amongst species did not correspond with the divergence of non-photochemical energy dissipation strategy but was generally consistent with the

relative dominance of species within the platform coral communities. Interpreting and fully understanding the nature of these fundamental photobiological properties will undoubtedly require a more detailed understanding of the mechanisms that regulate photobiological properties including the genetic composition of the algal symbionts and light absorption by the coral holobiont. Furthermore, a more detailed understanding of the inherent environmental variability over scales from days to seasons (e.g. Anthony et al. 2004; Piniak and Storlazzi 2008) will be key to further linking the mechanistic drivers of these properties, including those associated with stress tolerance, with the marginal conditions.

**Acknowledgments** The authors wish to thank the Captain and crew of RV *Moriá* for assistance in sampling. Also, the mission scientists and Principal Investigators who provided the GIOVANNI Ocean colour Radiometry (SeaWiFS) data used in this research effort as well as Dr. Bert Hoeksema for his discussions on coral endemism. This work was supported by an international travel grant from the Royal Society to DJSu. RPKP and MDMO were supported with funding from the Brazilian National Council for the Scientific and Technological Development (CNPq) and Fellowships (PQ2 and PD, respectively). We are also extremely thankful for invaluable comments from 3 anonymous reviewers thereby improving upon an earlier draft.

## References

- Anthony KRN, Connolly SR (2004) Environmental limits to growth: physiological niche boundaries of corals along turbidity-light gradients. *Oecologia* 141:373–384
- Anthony KRN, Hoegh-Guldberg O (2003) Kinetics of photoacclimation in corals. *Oecologia* 134:23–31
- Anthony KRN, Ridd PV, Orpin AR, Lacombe P, Lough J (2004) Temporal variation of light availability in coastal benthic habitats: Effects of clouds, turbidity, and tides. *Limnol Oceanogr* 49:2201–2211
- Aronson R, Bruckner A, Moore J, Precht B, Weil E (2008) *Siderastrea stellata*. In: IUCN 2011. IUCN Red List of Threatened Species v2011.2. [www.iucnredlist.org](http://www.iucnredlist.org). Accessed 13 Jan 2012
- Barnes DJ, Lough JM (1989) The nature of skeletal density banding in scleractinian corals: fine banding and seasonal patterns. *J Exp Mar Biol Ecol* 126:119–134
- Brown BE, Ambarsari I, Warner ME, Fitt WK, Dunne RP, Gibb SW, Cummings DG (1999) Diurnal changes in photochemical efficiency and xanthophyll concentrations in shallow water reef corals: evidence for photoinhibition and photoprotection. *Coral Reefs* 18:99–105
- Castro CB, Pires DO (2001) Brazilian coral reefs: what we already know and what is still missing. *Bull Mar Sci* 69:357–371
- Castro CB, Segal B, Pires DO, Medeiros MS (2005) Distribution and diversity of coral communities in the Abrolhos reef complex, Brazil. In: Dutra GF, Allen GR, Werner T, McKenna SA (Eds) A rapid marine biodiversity assessment of the Abrolhos Bank, Bahia, Brazil. RAP Bulletin of Biological Assessment 38. Conservation International, Washington DC, pp 19–39
- Cosgrove J, Borowitzka MA (2010) Chlorophyll fluorescence terminology: an introduction. In: Suggett DJ, Prasil O, Borowitzka MA (eds) *Chlorophylla fluorescence in aquatic sciences: methods and applications*. Springer, Berlin, pp 1–18
- Costa CF, Sassi R, Amaral FD (2004) Population density and photosynthetic pigment content in symbiotic dinoflagellates in the Brazilian scleractinian coral *Montastrea cavernosa* (Linnaeus, 1767). *Braz J Oceanogr* 52:93–99
- Costa CF, Sassi R, Amaral FD (2005) Annual cycle of symbiotic dinoflagellates from three species of scleractinian corals from coastal reefs of northeastern Brazil. *Coral Reefs* 24:191–193
- Costa CF, Sassi R, Amaral FD (2008) Zooxanthellae genotypes in the coral *Siderastrea stellata* from coastal reefs in northeastern Brazil. *J Exp Mar Biol Ecol* 367:149–152
- Devlin MJ, Barry J, Mills DK, Gowen RJ, Foden J, Sivyer D, Tett P (2008) Relationships between suspended particulate material, light attenuation and Secchi depth in UK marine waters. *Est Coast Shelf Sci* 79:429–439
- Dutra LXC, Kikuchi RKP, Leão ZMAN (2006) Effects of sediment accumulation on reef corals from Abrolhos, Bahia Brazil. *J Coastal Res* SI39:633–638
- Falkowski PG, Dubinsky Z (1981) Light-shade adaptation of *Stylophora pistillata*, a hermatypic coral from the Gulf of Eilat. *Nature* 289:172–174
- Fukami H, Chen CA, Budd AF, Collins A, Wallace C, Chuang YY, Chen C, Dai CF, Iwao K, Sheppard C, Knowlton K (2008) Mitochondrial and nuclear genes suggest that stony corals are monophyletic but most families of stony corals are not (Order Scleractinia, Class Anthozoa, Phylum Cnidaria). *PLoS ONE* 3:e3222. doi:10.1371/journal.pone.0003222
- Gorbunov MY, Kolber ZS, Lesser MP, Falkowski PG (2001) Photosynthesis and photoprotection in symbiotic corals. *Limnol Oceanogr* 46:75–85
- Hennige SJ, Smith DJ, Perkins R, Consalvey M, Patterson DM, Suggett DJ (2008) Photoacclimation, growth and distribution of massive corals in clear and turbid waters. *Mar Ecol Prog Ser* 369:77–88
- Hennige SJ, Suggett DJ, Smith DJ, McDougall K, Warner (2009) Photoacclimation of symbiotic dinoflagellates revisited: Bio-optical and biophysical signatures. *Coral Reefs* 28:179–191
- Hennige SJ, Walsh SJ, McGinly M, Smith DJ, Warner ME, Suggett DJ (2010) Coral acclimation and adaptation along an environmental gradient of an Indonesian reef complex. *J Exp Mar Biol Ecol* 391:143–152
- Hill R, Ralph PJ (2008) Dark-induced reduction of the plastoquinone pool in zooxanthellae of scleractinian corals and implications for measurements of chlorophyll a fluorescence. *Symbiosis* 46:45–56
- Jassby AT, Platt T (1976) Mathematical formulation of the relationship between photosynthesis and light for phytoplankton. *Limnol Oceanogr* 21:540–547
- Kikuchi RKP, Leão ZMAN, Oliveira MDM (2010) Conservation status and spatial patterns of AGGRA vitality indices in southwestern Atlantic reefs. *Rev Biol Trop* 58:1–31
- Kleypas JA, McManus JW, Menez LAB (1999) Environmental limits to coral reef development: where do we draw the line? *Am Zool* 39:146–159
- Knutson RA, Buddemeier RW, Smith SV (1972) Coral chronometers: seasonal growth bands in reef corals. *Science* 177:270–272
- Krug LA, Gherardi DFM, Stech JL, Leão ZMAN, Kikuchi RKP (2012) Characterization of coral bleaching environments and their variation along the Bahia state coast, Brazil. *Int J Rem Sens* 33:4059–4074
- Lavada J, Strzepek RF, Kroth PG (2007) Photoprotection capacity differs among diatoms: possible consequences on the spatial distribution of diatoms related to fluctuations in the underwater light climate. *Limnol Oceanogr* 52:1188–1194

- Leão ZMAN, Dominguez JML (2000) Tropical coast of Brazil. Mar Poll Bull 41:112–122
- Leão ZMAN, Kikuchi RKP (2005) A relic fauna threatened by global changes and human activities, Eastern Brazil. Mar Poll Bull 51:599–611
- Leão ZMAN, Kikuchi RKP, Testa V (2003) Corals and coral reefs of Brazil. In: Cortés J (ed) Latin American coral reefs. Elsevier, Amsterdam, pp 9–52
- Leão ZMAN, Kikuchi RKP, Oliveira MDM (2008) Coral bleaching in the reefs of Bahia and the relationship to anomalous events of sea surface temperature. Biota Neotropica 8:69–82
- Lesser MP, Slattery M, Stat M, Ojimi M, Gates RD, Grottoli A (2010) Photoacclimatization by the coral *Montastraea cavernosa* in the mesophotic zone: light, food, and genetics. Ecology 91:990–1003
- Oliver TA, Palumbi SR (2011) Do fluctuating temperature environments elevate coral thermal tolerance? Coral Reefs 30:429–440
- Piniak GA, Storlazzi CA (2008) Diurnal variability in turbidity and coral fluorescence on a fringing reef flat: Southern Molokai, Hawaii. Est Coast Shelf Sci 77:56–64
- Ralph PJ, Gademann R, Larkum AWD, Schreiber U (1999) In situ underwater measurements of photosynthetic activity of coral zooxanthellae and other reef-dwelling dinoflagellate endosymbionts. Mar Ecol Prog Ser 180:139–147
- Segal B, Evangelista H, Kampel M, Goncalves AC, Polito PS, dos Santos EA (2008) Potential impacts of polar fronts on sedimentation processes at Abrolhos coral reef (South-West Atlantic Ocean/Brazil). Cont Shelf Res 28:533–544
- Smith DJ, Etienne M, Spring N, Suggett DJ (2008) Tolerance, refuge and recovery of coral communities to thermal bleaching: evidence from reefs of the Seychelles. Proceedings of 11th international coral reef symposium, pp 398–402
- Suggett DJ, Smith DJ (2011) Interpreting the sign of coral bleaching: friend vs foe. Global Change Biol 17:45–55
- Suggett DJ, Oxborough K, Baker NR, MacIntyre HL, Kana TM, Geider RJ (2003) Fast repetition rate and pulse amplitude modulation chlorophyll a fluorescence measurements for assessment of photosynthetic electron transport in marine phytoplankton. Euro J Phycol 38:371–384
- Suggett DJ, MacIntyre HL, Geider RJ (2004) Evaluation of biophysical and optical determinations of light absorption by photosystem II in phytoplankton. Limnol Oceanogr Methods 2:316–332
- Suggett DJ, Moore CM, Hickman AE, Geider RJ (2009) Interpretation of fast repetition rate (FRR) fluorescence: signatures of community structure v physiological state. Mar Ecol Prog Ser 376:1–19
- Suggett DJ, Moore CM, Geider RJ (2010) Estimating aquatic primary productivity using active fluorescence. In: Suggett DJ, Prasil O, Borowitzka MA (eds) Chlorophylla fluorescence in aquatic sciences: methods and applications. Springer, Berlin, pp 103–127
- Warner ME, Lesser MP, Ralph PJ (2010) Chlorophyll fluorescence in reef building corals. In: Suggett DJ, Prasil O, Borowitzka MA (Eds) Chlorophylla fluorescence in aquatic sciences: methods and applications. Springer, Berlin, pp 209–222
- Yentsch CS, Yentsch CM, Cullen JJ, Lapointe B, Phinney DA, Yentsch SW (2002) Sunlight and water transparency: cornerstones in coral research. J Expt Mar Biol Ecol 268:171–183